ISSN 1063-4576, Journal of Superhard Materials, 2021, Vol. 43, No. 6, pp. 415–422. © Allerton Press, Inc., 2021.
Ukrainian Text © The Author(s), 2021, published in Nadtverdi Materialy, 2021, Vol. 43, No. 6, pp. 47–57.

PRODUCTION, STRUCTURE, PROPERTIES

Microstructure and Mechanical Properties of c-BN Reinforced (Ti,W)C-Based Cermet Tool Materials

Bin Fang[a], *, Zhonghang Yuan[a], Liying Gao[a], Depeng Li[a], and Yuanbin Zhang[a]

[a] *School of Mechanical and Automotive Engineering, Qilu University of Technology (Shandong Academy of Sciences), Jinan, 250353 China*

**e-mail: fb@qlu.edu.cn*

Received January 30, 2020; revised June 2, 2021; accepted August 10, 2021

Abstract—(Ti,W)C-based cement tool materials with c-BN particles as additive phase are fabricated by the hot press sintering. The effect of c-BN addition on the microstructure and mechanical properties of (Ti,W)C-based cement tool materials are investigated. With the addition of c-BN, the fracture mode of composite transform from intergranular to transgranular fracture. The main toughening mechanism is particle bridging, crack deflection and crack bifurcation, which improve the fracture toughness of cement tool material. The proper addition of c-BN can improve the mechanical properties of the composites. When the content of c-BN is 1.5 wt %, (Ti,W)C-based cement tool materials reaches the optimum comprehensive mechanical properties. The hardness, the flexural strength and the fracture toughness is 19.78 GPa, 987 MPa and 9.44 MPa $m^{1/2}$, respectively.

Keywords: c-BN, cements, hot pressing sintering, mechanical properties, microstructure

DOI: 10.3103/S1063457621060046

1. INTRODUCTION

Cermets are the important engineering composites and have been used for cutting tools, abrasive slurry nozzles, mechanical seal rings, bearings, and forming dies because of their high mechanical properties, outstanding wear and oxidation resistance and thermal stability. Cermets are composed of ceramic phase which provides high hardness and metal binder phase which bonds the ceramic phase and contributes to toughness and ductility. Ceramic phases have carbides, nitrides, oxides, carbonitrides of titanium, molybdenum, tungsten, and tantalum, while cobalt, nickel, molybdenum alloys, etc., are usually applied as the metal binder [1, 2].

(Ti,W)C-based carbides are generally fabricated by liquid phase sintering, whose hard phase is dispersed in tough metal binder phase. The relevant studies showed that the mechanical properties can be improved by the optimized composites and the surface treatment. (Ti,W)C-based cemented carbides with 15 wt % Co binder phase have the best comprehensive mechanical properties [3]. Nam [4] found that the toughness of (Ti,W)C–Co hard materials is enhanced by the additive of a thin platelet (Ti,W)C phase. Lin [5] found that Mo_2C additive can improve the sinterability and the mechanical properties of (Ti,W)C. Chen [6] reported that finer microstructures were obtained and the hardness and transverse rupture strength of (Ti,W,Ta)C improved with the increase of Mo addition. Prokopiv [7–11] found out that thermal compression treatment of WC–(Ti,W)C–Co cemented carbide reduces residual microporosity, eliminates pores and has the formation of the elongated-shape phase in the microstructure, which is benefit for the improvement of the tool life and cutting properties. WC–(Co,Ni,Al) film, improving the operational properties, can be formation with the Ni_3Al and the WC–7(W,Ti)C–10Co cemented carbide at 1530°C in a vacuum on the cutting plate surface [12]. (Ti,W)C-based carbides are usually used for tool materials in high-speed machining, semi-finishing, and finishing work for both carbon and stainless steels [4, 13–16]. The fracture toughness of tool materials is one of the most important factor for the life and reliability of cutting tools. Meanwhile, the wettability is poor between (Ti,W)C hard phase and Co binder phase, which leads to low densification, abnormal grain growth and degradation of the mechanical properties during sintering [5, 14]. In order to improve the strength and fracture toughness of ceramic-matrix composites, various toughening methods was developed, such as platelet strengthening [17], whisker reinforcements [18, 19], grain bridging [20], and second-phase particle toughing [21, 22].

Table 1. Characteristics of raw powders

Powders	Particle size, μm	Theoretical density, g/cm^3	Thermal expansion, 10^{-6} K^{-1}	Elastic modulus, GPa
$(Ti_{0.5},W_{0.5})C$	1–3	9.49	5.58	570
c-BN	0.1–0.3	3.49	4.7	700
Co	1–3	8.9	6.8	213

Table 2. The content of cermet tool materials (wt %)

Samples	(Ti,W)C	Co	c-BN
CT0	85	15	0
CT1	84	15	1.0
CT1.5	83.5	15	1.5
CT2	83	15	2.0
CT3	82	15	3.0

The cemented carbides with the additive second-phase have attracted much attention because the second-phase particles could enhance wettability and sinterability, impede grain growth and improve microstructure. It is well known that the mechanical properties of cemented carbides are close related with their microstructure. The addition of the second phase particles in the material can effectively improve the mechanical properties of the composites [23–26]. Cubic boron nitride (c-BN) has the second greatest hardness and is less reactive with ferrous materials, which makes it the appropriate enforcing additive phase for the tool material in material removal applications for ferrous workpieces [27]. c-BN is applied to the preparation of various composite tool materials, such as Al_2O_3–cBN, β-Sialon–cBN, TiN–cBN, mullite–cBN and other composite tool materials [28–32]. Zhang et al. [33] studied WC–Co–c-BN composites and found that the additive of c-BN can improve the Vickers hardness and fracture toughness of the material. Chiou et al. [34] studied the effects of c-BN contents on the mechanical properties of c-BN/TiC composite ceramics and found that the Vickers hardness of the ceramic composites was the highest at the molar ratio of c-BN/TiC of 2 : 1. Zhang et al. [35] proposed that c-BN improve the mechanical properties of Ti(C,N)-based cermet. Klimczyk et al. [36] fabricated Al_2O_3–c-BN composites by spark plasma sintering (SPS) and high pressure high temperature (HPHT) and found that the relative density and Vickers hardness of the composites prepared by SPS were slightly lower than those prepared by HPHT. The improvement of c-BN@Al_2O_3 as the additive on the microstructure and mechanical was investigated by our group [37]. However, the preparation of c-BN@Al_2O_3 is complicated and time-cost. It is also useful to analyse the effect of c-BN without surface modification on the grain growth and material performance of (Ti,W)C-based cement composites for the development of the novel type cermet tool materials.

In this paper, to explore the effects of c-BN addition on the grain growth and material performance of (Ti,W)C-based cement composites, (Ti,W)C-based cement tool materials was fabricated by using (Ti,W)C as matrix, Co as binder, c-BN particles as additive phase by the hot press sintering. The influence of the c-BN addition on the microstructure, grain size, fracture mode and mechanical properties of (Ti,W)C-based cermets were investigated.

2. EXPERIMENTAL

The particle sizes, stoichiometries and oxygen contents of the raw powders used are given in Table 1. The content of cermet tool material is shown in Table 2. The c-BN powder was dispersed with sodium dodecyl sulfate as a modifier in order to prevent its agglomeration. The pre-weighted $(Ti_{0.5},W_{0.5})C$, c-BN, Co and WC powders were mixed in the anhydrous alcohol by the mechanical milling with WC–Co balls for 48 h at the speed of 70 rpm and the ball-to-powder ratio of 10 : 1. The tool materials was fabricated by hot pressing sintering with the mixed powders. The sintering temperature, holding time and sintering pressure were 1450°C, 60 min and 30 MPa, respectively. The dimensions of the specimen is 3 × 4 × 30 mm.

Archimedes' method was employed to measure the density of the sintered compact. The microstructure of the material was observed using an emission scanning electron microscope (SEM). EDS mapping

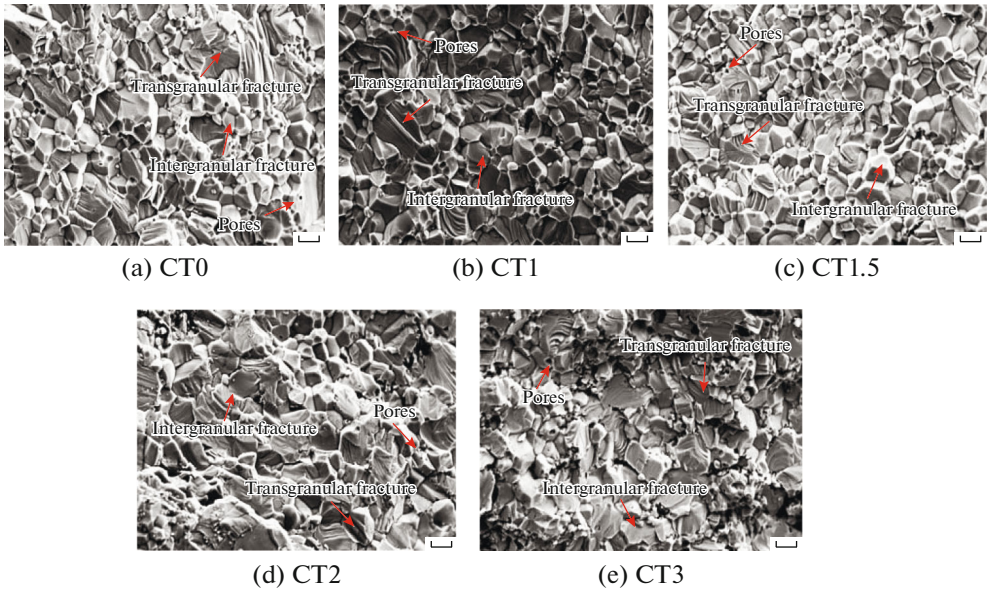

(a) CT0 (b) CT1 (c) CT1.5

(d) CT2 (e) CT3

Fig. 1. Fracture morphologies of cement tool materials for the different contents of c-BN.

was used to analyze the composition of the sample. The grain sizes of (Ti,W)C-based cermets were determined using ImageJ based on the SEM images. More than 200 particles were measured to obtain statistically meaningful results. The flexural strength was measured by the three-point bending method. The hardness was investigated with a load of 300 N and a holding time of 15 s. The fracture toughness (K_{IC}) was calculated using the following expression [38]:

$$K_{IC} = 0.15\left(\frac{H_{v30}}{\sum_{i=1}^{4} l_i}\right)^{1/2}, \quad (1)$$

where H_{v30} is the Vicker's hardness (N/mm^2) under 300 N, l_i is the length of the crack tip from the hardness indent (mm).

3. RESULTS AND DISCUSSION

3.1. Microstructure

Figure 1 is the fracture morphologies of (Ti,W)C-based cement tool materials with the different c-BN content. The sintering temperature, holding time and sintering pressure are 1450°C, 60 min and 30 MPa, respectively. The occurrence of a mixed intergranular-transgranular fracture mode was found from the fracture surfaces. The fracture steps can be found at many positions, which is the typical micromorphology feature of the transgranular fracture. Smooth grain boundaries can be also found, which is the significant micromorphology feature of the intergranular fracture. It can be seen from Fig. 1 that the micromorphology feature of the transgranular fracture which has c-BN phase is more than that which has no c-BN phase. The fracture mode of Figs. 1b, 1c is mainly the transgranular fracture, accompanied by the intergranular fracture. In the process of fracture, more fracture energy will be consumed by the transgranular fracture, and the mechanical properties of the composites will be enhanced.

It was also observed that the microstructure of the cemented carbides varied in porosity, agglomeration status and particle sizes. The microstructure of the composites with no c-BN phase in Fig. 1a significantly exists the abnormal growth grain and the gain size is uneven. Comparing with Figs. 1a–1e, the most uniform distribution of particles in the composites was obtained with the c-BN content of 1.5 wt %.

It is shown in Fig. 1 that the number of voids is smallest in Fig. 1c, which indicates the influence of the content of c-BN on the densification process. The microstructure has an important influence on the fracture behavior of the composite. Comparing Fig. 1c with Figs. 1a, 1b, 1d, 1e, not only the number of pores

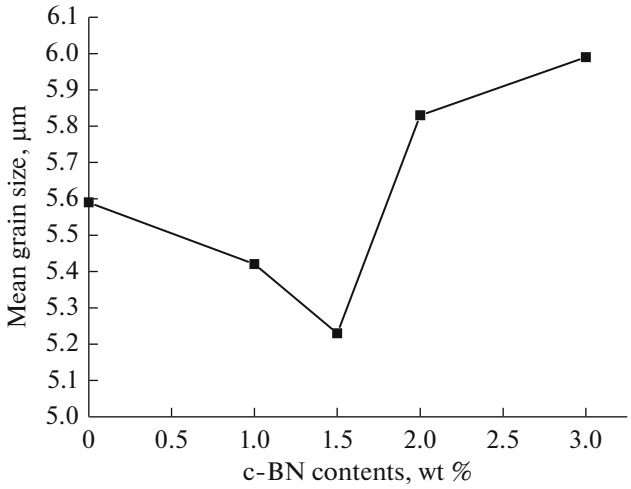

Fig. 2. Mean grain size for the different contents of c-BN.

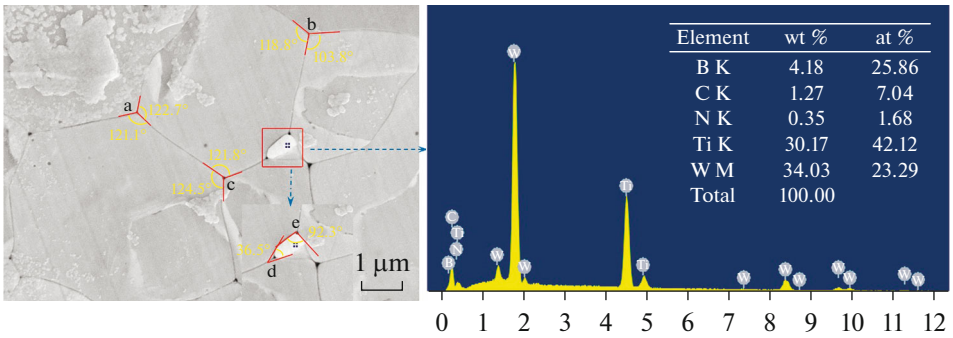

(a) SEM morphology of the etched surface (b) EDS mapping

Fig. 3. SEM images and EDS mapping of the etched surface of CT1.5.

is least, but also the grain size is the most uniform in Fig. 1c, which can enhance the mechanical properties of composite materials.

Compared with the microstructure in Fig. 1, the grain size in Fig. 1c is smallest. The mean grain sizes for the different contents of c-BN were obtained by using ImageJ software, as shown in Fig. 2. It was observed that the mean gain size decreases firstly and then increases. The minimum mean grain size of CT1.5 is 5.23 μm and the maximum mean grain size of CT3 is 5.99 μm, which implied the proper content additive to impede the grain growth and refine the grain. However, excessive additive is not beneficial to grain refinement during sintering. Grains grow (or shrink) by the addition (or removal) of atoms that are transported to (or away from) the grain by capillary driven diffusion, which lead to the change in the position of a grain boundary as volume is transferred from one grain to another. The second particles can impede the mobility of boundary. In order to further investigate the effect of c-BN on the microstructure, the EDS mapping of the etched surface of CT1.5 are given in Fig. 3. As shown in Figs. 3a, 3b, B and N elements are found, which indicates that the grain is c-BN. c-BN particle lies in triple junction, which can hinder (Ti,W)C grain growth during the sintering. According to the von Neumann-Mullins rule for growth in two-dimensional systems, the angles among the triple truncation follow the Eq. 2 when the boundary equilibrium is reached during grain growth [39, 40].

$$\frac{\gamma_{1-2}}{\sin\alpha_1} = \frac{\gamma_{2-3}}{\sin\alpha_2} = \frac{\gamma_{1-3}}{\sin\alpha_3}, \tag{2}$$

where α_n are the dihedral angles between boundaries and γ_{n-m} are the specific surface energies. As long as the grain boundary energies are isotropic, the dihedral angles of the equilibrium of grain growth are 120°.

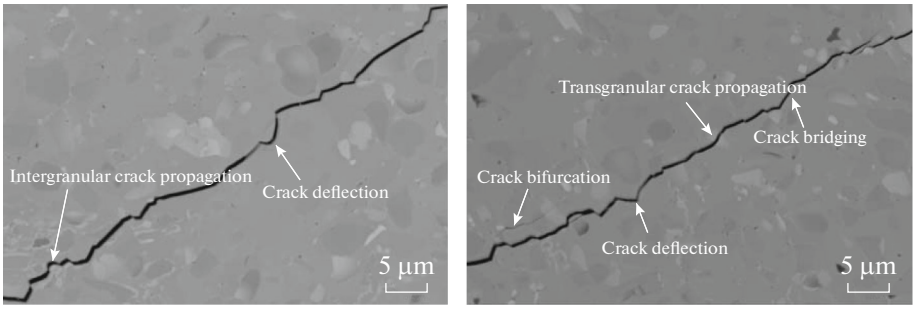

(a) CT0 (b) CT1.5

Fig. 4. Crack propagation for the different contents of c-BN (SEM).

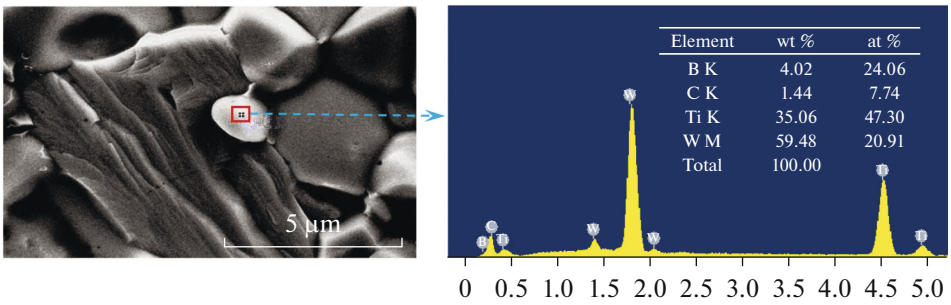

(a) SEM morphology of the fracture surface (b) EDS mapping

Fig. 5. SEM and EDS mapping of the fracture surface of CT1.5.

As shown in Fig. 3a, the dihedral angles of point a, b and c are approximately 120°, which indicates that the boundary equilibrium is reached. However, the dihedral angles of point e and f are 36.5° and 92.3°, respectively, which means that the boundary equilibrium is not reached because of the inhibition of c-BN particle during the sintering. The evolution of grain size and microstructure is governed largely by grain boundary migration process during sintering. The second particles can inhibit the grain growth which is named Zener pinning, can affect grain-boundary migration behavior and can change the grain-growth rate [41, 42]. c-BN particle as the pinning particles which lies in the triple joint can inhibit the grain boundary migration and slow down the grain growth, which is beneficial to the grain refinement.

According to the Hall-Petch principle, $\sigma = \sigma_0 + Kd^{-\frac{1}{2}}$, where σ is the yield stress; σ_0 is the lattice friction resistance generated when moving a single dislocation; K is a constant; and d is the mean grain diameter. The reduction in the grain size can significantly improve the mechanical properties of cermet tool materials.

Figure 4 shows the crack propagation of CT0 and CT1.5. It is observed that there is the intergranular crack propagation and crack deflection in Fig. 4a. Comparing with Fig. 4b, it is also found in Fig. 4a the path of the crack propagation is straighter, which is without c-BN particles. When c-BN particles are encountered in the crack propagation process, it tends to crack bifurcation, crack bridging, tansgranular crack propagation and crack deflection which are beneficial to the improvement of the mechanical properties of the (Ti,W)C-based cemented carbides.

Figure 5 shows the SEM micrographs and EDS analysis results of the fracture surface of CT1.5. As shown in Figs. 5a, 5b, B element was found, which indicates that the grain is c-BN particle. There exists the transgranular fracture mode around c-BN particle. It is further proven that the fracture mode is prone to change from the intergranular fracture to the transgranular fracture because of the effect of c-BN particle.

3.2. Density and Mechanical Properties

3.2.1. Material density. The effect of c-BN content on the volume density and relative density of (Ti,W)C-based cement tool materials was shown in Fig. 6. With the increase of c-BN content, the volume

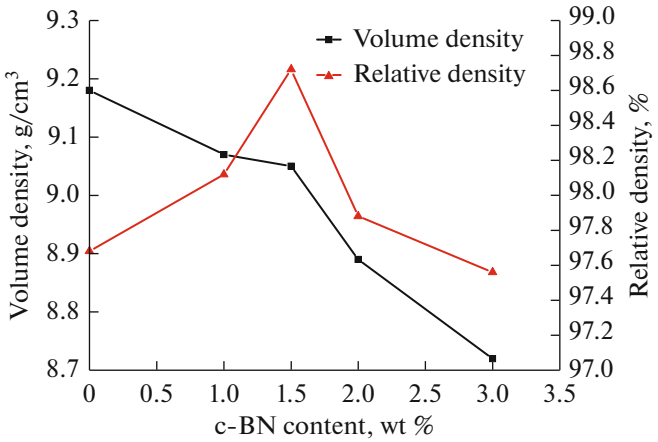

Fig. 6. Density and relative density of (Ti,W)C-based cement tool materials at different c-BN content.

density of (Ti,W)C-based cement tool materials decreased because the theoretical density of c-BN is only 3.49 g/cm^3. However, the relative density firstly increases and subsequently decreases. The relative density reaches the maximum of 98.72% when the content of c-BN is 1.5 wt %, which is good agreement with Fig. 1 because of the least number of pores in Fig. 1c. The relative density is affected by the amount of liquid present, contact angle, particle size and solubility of solid in the liquid sintering [44]. c-BN has small particle size and can be dissolved in the binder. The proper contents of c-BN contribute to the rearrangement and grain shape accommodation during the initial and intermediate stage in liquid sintering, which could lead to the pore elimination and increase the densification and the relative density of the tool materials. When the content of c-BN increases more than 1.5 wt %, the densification process is hindered because of the heavy agglomeration and the poor sinterability of c-BN, which results in a large number of pores and decreases in the relative density of the tool materials and is an good accordance with the microstructure as shown in Fig. 1e.

3.2.2. Mechanical properties. The hardness, flexural strength and fracture toughness of (Ti,W)C-based cement tool materials with different c-BN content are presented in Table 3. The hardness without the second phase is 17.74 ± 0.54 GPa. Compared with the hardness of (Ti,W)C-based cemented carbides without the second phase, the hardness of (Ti,W)C-based cemented carbides with c-BN particles is improved because of the influence of the second greatest hardness of c-BN particles. When the content of c-BN reaches 2 wt %, the hardness reaches the maximum value of 20.15 ± 0.61 GPa. CT1.5 materials shows the highest flexural strength and fracture toughness and the second greatest hardness, which have the good comprehensive mechanical properties. Compared with the CT0, the hardness, the flexural strength and the fracture toughness increases from 17.74 to 19.78 GPa, from 873 to 987 MPa, from 8.12 MPa m$^{1/2}$ to 9.44 MPa m$^{1/2}$, respectively. The increase rates of harness, flexural strength and fracture toughness are 11.5, 13.1 and 10.2%, respectively.

The mechanical properties of (Ti,W)C-based cement tool materials are significantly influenced by c-BN additives. When c-BN content is 1.5%, the optimum mechanical properties of (Ti,W)C-based cement tool materials is achieved, which is good consistent with the above analysis.

Table 3. Mechnical properties of cermet tool meaterials with different c-BN contents

Samples	Hardness, GPa	Flexural strength, MPa	Fracture toughness, MPa m$^{1/2}$
CT0	17.74 ± 0.54	73 ± 38	8.41 ± 0.28
CT1	18.76 ± 0.57	889 ± 32	8.52 ± 0.25
CT1.5	19.78 ± 0.52	987 ± 34	9.27 ± 0.2
CT2	20.15 ± 0.61	845 ± 43	8.82 ± 0.24
CT3	18.13 ± 0.58	815 ± 46	8.32 ± 0.26

4. CONCLUSIONS

(1) (Ti,W)C-based cermet tool meaterials with the different c-BN contents have been prepared by hot pressing sintering with the sintering temperature, holding time and sintering pressure of 1450°C, 60 min and 30 MPa respectively.

(2) c-BN particles can refine the grain effectively, improve the density and reduce the defects. With the addition of c-BN, the fracture form of composite can change from intergranular fracture to transgranular fracture.

(3) The addition of c-BN can significantly improve the mechanical properties of the composites. When c-BN content is 1.5%, (Ti,W)C-based cement tool materials possesses the optimum comprehensive mechanical properties. The hardness, the flexural strength and the fracture toughness is 19.78 GPa, 987 MPa and 9.44 MPa $m^{1/2}$, respectively.

FUNDING

This work was supported by National Natural Science Foundation of China (projects no. 51675289 and 52075275), Agricultural Key Applied Project of China (no. SD2019NJ015) and Project for the Innovation Team of Universities and Institutes in Jinan of China (no. 2018GXRC005).

CONFLICT OF INTEREST

The authors declare that they have no conflicts of interest.

AUTHOR CONTRIBUTIONS

Bin Fang: methodology, conceptualization, writing (review and editing), data curation, and general supervision. Zhonghang Yuan: writing (original draft). Depeng Li: resources, writing (review and editing), and data curation. Yuanbin Zhang: writing (editing).

REFERENCES

1. Aramian, A., Mohammad, J.R.S., Sadeghian, Z., and Berto, F., A review of additive manufacturing of cermets, *Addit. Manuf.*, 2020, vol. 33, pp. 1–17.
2. Buchholz, S., Farhat, Z.N., Kipouros, G.J., and Plucknett, K.P., The reciprocating wear behavior of TiC–Ni_3Al cermets, *Int. J. Refract. Met. Hard Mater.*, 2012, vol. 33, pp. 44–52.
3. Daoush, W.M., Lee, K.H., Park, H.S., and Hong, S.H., Effect of liquid phase composition on the microstructure and properties of (W,Ti)C cemented carbide cutting tools, *Int. J. Refract. Met. Hard Mater.*, 2009, vol. 27, no. 1, pp. 83–89.
4. Nam, H., Lim, J., and Kang, S., Microstructure of (W,Ti)C–Co system containing platelet WC, *Mater. Sci. Eng., A*, 2010, vol. 527, nos. 27–28, pp. 7163–7167.
5. Lin, Z., Xiong, J., Guo, Z., Zhou, W., Wan, W., and Yang, L., Effect of Mo_2C addition on the microstructure and fracture behavior of (W,Ti)C-based cemented carbides, *Ceram. Int.*, 2014, vol. 40, no. 10, pp. 16421–16428.
6. Chen, X., Xiong, W., Qu, J., Yang, Q., Yao, Z., and Huang, Y., Microstructure and mechanical properties of (Ti,W,Ta)C-*x*Mo-Ni cermets, *Int. J. Refract. Met. Hard Mater.*, 2012, vol. 31, pp. 56–61.
7. Prokopiv, N.M., Kharchenko, O.V., Tkach, S.V., Vasilenko, L.E., Prokopiv, N.N., Serdyuk, Y.D., and Semizhon, O.A., The influence of thermal-compression treatment under argon pressure of 3.0 MPa on microstructure of standard (Ti, W)C–WC–10Co hardmetal, *J. Superhard Mater.*, 2011, vol. 33, no. 5, pp. 320–326.
8. Serdyuk, Y.D., Semizhon, O.A., Prokopiv, N.M., Petasyuk, G.A., Kharchenko, O.V., and Omel'chuk, T.V., The influence of thermal compression treatment parameters on quality characteristics and wear mechanisms of T5K10 carbide inserts in rough turning, *J. Superhard Mater.*, 2011, vol. 33, no. 2, pp. 120–128.
9. Prokopiv, M.M., A new phenomenon in the structure formation of T5K10 hard alloy, *J. Superhard Mater.*, 2018, vol. 40, no. 1, pp. 73–74.
10. Prokopiv, M.M., A study of new phase of elongated shape in granular structure of WC–(Ti,W)C–Co cemented carbide after its solid-phase annealing, *Int. J. Refract. Met. Hard Mater.*, 2020, vol. 93, 105349.
11. Prokopiv, M., Metallographic studies of extra elongated inclusions in WC–(Ti,W)C–Co hard alloy structure, *J. Mater. Sci. Appl.*, 2019, Vol. 5, no. 2, pp. 29–34.
12. Prokopiv, M.M., Formation of layer WC–(Co,Ni,Al) structure on the cutting plate surface of WC–7(W,Ti)C–10Co cemented carbide in the contact area with Ni_3Al melt, *J. Superhard Mater.*, 2019, vol. 41, no. 3, pp. 149–156.
13. Kwon, H., Suh, C.Y., and Kim, W., Microstructure and mechanical properties of (Ti,W)C–Ni cermet prepared using a nano-sized TiC–WC powder mixture, *J. Alloy Compd.*, 2015, vol. 639, pp. 21–26.
14. Zhang, G., Xiong, W., Yang, Q., Yao, Z., Chen, S., and Chen, X., Effect of Mo addition on microstructure and mechanical properties of (Ti,W)C solid solution based cermets, *Int. J. Refract. Met. Hard Mater.*, 2014, vol. 43, pp. 77–82.

15. Qu, J., Xiong, W., Ye, D., Yao, Z., Liu, W., and Lin, S., Effect of WC content on the microstructure and mechanical properties of $Ti(C_{0.5}N_{0.5})$–WC–Mo–Ni cermets, *Int. J. Refract. Met. Hard Mater.*, 2010, vol. 28, no. 2, pp. 243–249.
16. Jung, J. and Kang, S., Sintered (Ti,W)C carbides, *Scr. Mater.*, 2007, vol. 56, no. 7, pp. 561–564.
17. Xiong, H., Guo, Y., Li, Z., and Zhou, K., New production of (Ti,W)C-based cermets toughened by in-situ formed WC and twinned (Ti,W)C platelets: Carbonization of the $Ni_x(Ti_{0.6},W_{0.4})_4C$-type η phases, *J. Alloy Compd.*, 2018, vol. 731, pp. 253–263.
18. Zhao, B., Liu, H., Huang, C., Wang, J., and Cheng, M., Fabrication and mechanical properties of Al_2O_3–SiC_w–TiC_{np} ceramic tool material, *Ceram. Int.*, 2017, vol. 43, no. 13, pp. 10224–10230.
19. Liu, X., Liu, H., Huang, C., Zhao, B., and Zheng, L., High temperature mechanical properties of Al_2O_3-based ceramic tool material toughened by SiC whiskers and nanoparticles, *Ceram. Int.*, 2017, vol. 43, no. 1, pp. 1160–1165.
20. Tian, X., Zhao, J., Zhu, N., Dong, Y., and Zhao, J., Preparation and characterization of Si_3N_4/(W,Ti)C nanocomposite ceramic tool materials, *Mater. Sci. Eng., A*, 2014, vol. 596, pp. 255–263.
21. Rafiaei, S.M., Kim, J.H., and Kang, S., Effect of nitrogen and secondary carbide on the microstructure and properties of $(Ti_{0.93}W_{0.07})$C–Ni cermets, *Int. J. Refract. Met. Hard Mater.*, 2014, vol. 44, pp. 123–128.
22. Song, J., Huang, C., Zou, B., Liu, H., and Wang, J., Microstructure and mechanical properties of TiB_2–TiC–WC composite ceramic tool materials, *Mater. Des.*, 2012, vol. 36, pp. 69–74.
23. Xie, Y. and Koslowski, M., Numerical simulations of inter-laminar fracture in particle-toughened carbon fiber reinforced composites, *Composites, Part A*, 2017, vol. 92, pp. 62–69.
24. Kang, X., Lin, N., He, Y., and Zhang, M., Influence of ZrC addition on the microstructure, mechanical properties and oxidation resistance of Ti(C,N)-based cermets, *Ceram. Int.*, 2018, vol. 44, no. 10, pp. 11151–11159.
25. Li, Y., Liu, N., Zhang, X., and Rong, C., Effect of WC content on the microstructure and mechanical properties of (Ti,W)(C, N)–Co cermets, *Int. J. Refract. Met. Hard Mater.*, 2008, vol. 26, no. 1, pp. 33–40.
26. Sandoval, D.A., Roa, J.J. Ther, O., Tarrés, E., and Llanes, L., Micromechanical properties of WC–(W,Ti,Ta,Nb)C–Co composites, *J. Alloy Compd.*, 2019, vol. 777, pp. 593–601.
27. Klimczyk, P., Cura, M.E., Vlaicu, A.M., Mercioniu, I., Wyżga, P., Jaworska, L., and Hannula, S.P., Al_2O_3–cBN composites sintered by SPS and HPHT methods, *J. Eur. Ceram. Soc.*, 2016, vol. 36, no. 7, pp. 1783–1789.
28. Hotta, M. and Goto, T., Densification and microstructure of Al_2O_3–cBN composites prepared by spark plasma sintering, *J. Ceram. Soc. Jpn.*, 2008, vol. 116, no. 6, pp. 744–748.
29. Hotta, M. and Goto, T., Densification and phase transformation of β-sialon–cubic boron nitride composites prepared by spark plasma sintering, *J. Am. Ceram. Soc.*, 2009, vol. 92, no. 8, pp. 1684–1690.
30. Hotta, M. and Goto, T., Spark plasma sintering of TiN–cubic BN composites, *J. Ceram. Soc. Jpn.*, 2010, vol. 118, no. 2, pp. 137–140.
31. Turkevich, D., Bushlya, V., Petrusha, I., Belyavina, N., Turkevich, V., and Ståhl, J.-E., HP-HT sintering, microstructure, and properties of B_6O- and TiC-containing composites based on cBN, *J. Superhard Mater.*, 2015, vol. 37, pp. 143–154.
32. Slipchenko, K.V., Petrusha, I.A., Stratiichuk, D.A., and Turkevych, V.Z., The influence of VC–Al additive on wear resistance of cBN-based composites, *J. Superhard Mater.*, 2018, vol. 40, no. 3, pp. 226–227.
33. Zhang, J., Tu, R., and Goto, T., Spark plasma sintering and characterization of WC–Co–cBN composites, *Key Eng. Mater.*, 2014, vol. 616, pp. 194–198.
34. Chiou, S.Y., Ou, S.F., Jang, Y.G., and Ou, K.L., Research on CBN/TiC composites, Part 1: Effects of the cBN content and sintering process on the hardness and transverse rupture strength, *Ceram. Int.*, 2013, vol. 39, no. 6, pp. 7205–7210.
35. Zhang, H., Gu, S., and Yi, J., Fabrication and properties of Ti(C,N) based cermets reinforced by nano-CBN particles, *Ceram. Int.*, 2012, vol. 38, no. 6, pp. 4587–4591.
36. Klimczyk, P., Cura, M.E., Vlaicu, A.M., Mercioniu, I., Wyżga, P., Jaworska, L., and Hannula, S.P., Al_2O_3–cBN composites sintered by SPS and HPHT methods, *J. Eur. Ceram. Soc.*, 2016, vol. 36, no. 7, pp. 1783–1789.
37. Fang, B., Li, D., Yi, M., Zhang, G., Xiao, G., Chen, Z., Zhang, J., and Xu, C., Effect of c-BN surface modification on the microstructure and mechanical properties of (Ti,W)C-based cermet tool materials, *Ceram. Int.*, 2020, vol. 46, no. 8, pp. 12145–12155.
38. Schubert, W.D., Neumeister, H., Kinger, G., and Lux, B., Hardness to toughness relationship of fine-grained WC–Co hard metals, *Int. J. Refract. Met. Hard Mater.*, 1998, vol. 16, pp. 133–142.
39. Blikstein, P. and Tschiptschin, A.P., Monte Carlo simulation of grain growth, *Mater. Res.*, 1999, vol. 2, no. 3, pp. 133–137.
40. Gottstein, G., Ma Y., and Shvindlerman, L., Triple junction motion and grain microstructure evolution, *Acta Mater.*, 2005, vol. 53, no. 5, pp. 1535–1544.
41. Miodownik, M., Martin, J.W., and Cerezo, A., Mesoscale simulation of particle pinning, *Philos. Mag. A*, 1999, vol. 79, no. 1, pp. 203–222.
42. Sterns, L. and Harmer, M., Particle-inhibited grain growth in Al_2O_3–SiC. I. Experimental results, *J. Am. Ceram. Soc.*, 1996, vol. 79, no. 12, pp. 3013–3019.
43. Upadhyaya, G.S., Materials science of cemented carbides-an overview, *Mater. Des.*, 2001, vol. 22, pp. 483–489.